View metadata, citation and similar papers at core.ac.uk

brought to you by CORE

provided by Elsevier - Publisher Connector

Available online at www.sciencedirect.com

ScienceDirect

Energy Procedia 57 (2014) 1878– 1887

Energy Procedia

2013 ISES Solar World Congress

Smart Switchable Technologies for Glazing and Photovoltaic Applications

P.Lemarchand[a]*, J.Doran[a], B.Norton[a]

[a]*Schoolof Physics, Dublin Energy Lab, Focas Institute, Dublin Institute of Technology,Camden Row,Dublin 8,Ireland*

Abstract

One presents in this paper an idea to use switchable technologies to independently control the solar heat flow and the visible light transmission through windows, and potentially collect infrared radiant power on a photovoltaic cell. The system uses chiral liquid crystal and suspended particle device switchable technologies that are electronically tuned to optically control the quantity of infrared light rejected, the visible light transmission and the optical path to internally reflect the light and collect it on the photovoltaic cell.

A characterized suspended particle device showed an average 48.5% to 1.3% transmission respectively in the transparent and opaque states of the window. A second characterization of a chiral liquid crystal mirror manufactured to reflect the visible range showed an average transmission modulation between 84% and 3% over 250nm reflection range respectively in the transparent and reflective states at small light incidence angles. Transmission is however significantly increasing in the reflective state while increasing light incidence angle and considered in ray-tracing simulation of the system.

A ray tracing software has been developed to simulate the performance of a window 50cm height by 50cm long and 5.5cm wide consisting of two chiral liquid crystal mirrors and using the characterization results. Adaptation of the mirrors configuration was considered to collect light on the cell at various zenith and azimuth solar angles.

Simulation results showed no significant benefit of internally reflecting the light to concentrate it on the photovoltaic cell located in the windows frame. However, an infrared chiral mirror with a reflection bandwidth wider than the wavelength range to modulate in transmission could potentially control solar heat radiation through the window between ~ 80% and 5% independently of the light incidence angle. The window system would technically benefit of a combined suspended particle device solely absorbing the visible range to realize the desired hybrid system.

© 2014 The Authors. Published by Elsevier Ltd. This is an open access article under the CC BY-NC-ND license (http://creativecommons.org/licenses/by-nc-nd/3.0/).

Selection and/or peer-review under responsibility of ISES.

Keyword: Switchable window, suspended particle device, chiral liquid crystal mirror

* Corresponding author. Tel.: +353-867267730

E-mail address: philippe.lemarchand@mydit.ie .

1876-6102 © 2014 The Authors. Published by Elsevier Ltd. This is an open access article under the CC BY-NC-ND license (http://creativecommons.org/licenses/by-nc-nd/3.0/).

Selection and/or peer-review under responsibility of ISES.

doi:10.1016/j.egypro.2014.10.052

1. Introduction

Switchable windows use either thermotropic, gasotropic or electrotropic technologies and find applications, among others, for building facades and vehicles to adapt solar transmission to the user's comfort. Among the electrochromic type, suspended particle devices (SPD) provide a fast switching uniform response of the absorption across a large window area. They have the additional advantage to provide a clear sight independently of the absorption state and absorb solar heat energy helping on reducing the cost associated with cooling and heating buildings [1,2,3,4]. Suspended particle device switchable windows enable electronic tuning of the light absorption by controlling the orientation of the rod-like particles. Absorption within the visible range then enables us to control the intensity of light transmission and glare through the window.

Switchable mirrors switch electronically between a reflective semi-opaque state and a nearly transparent state. Chiral liquid crystal (CLC) switchable mirrors have the advantage over prismatic, electrochromic, and gasochromic technologies of being industrially produced solid state devices with useful lives over ten years in indoor environments [5,6,7,8,9]. Previous measurements on a switchable mirror using a chiral liquid crystal technology manufactured to reflect the visible light range have shown that reflection up to 87% can be achieved in the mirror state. CLC switchable mirrors can be manufactured to reflect a spectral bandwidth from 50nm to 1000nm, in the range from 380nm to 3600nm.

Integrating both technologies in a window system comprised of CLC switchable mirrors and a suspended particle device switchable window could enable to control the visible light and solar infrared range independently. Solar energy heat transfer and visible glare could then be controlled independently. The proposed configuration integrates two facing CLC switchable mirrors and a SPD window. To use the rejected light by the CLC mirror, the back mirror may be tilted to increase the light incidence angle. This mirror could possibly act as a booster mirror for light that would then be collected by a photovoltaic cell optimized for the infrared and located in, or attached to, the window frame. Addressable pixels of the front mirror could allow adaption of the mirror configuration according to solar angles thus internally reflecting light to a cell to further increase light collection. Spectral reflection and transmission from CLC switchable mirrors are however dependent strongly on light incidence. Using a ray-tracing technique, the percentage of light being reflected, transmitted and absorbed by the system in addition to the percentage of light being transferred to the photovoltaic cell are calculated to assess the performance of such system.

Nomenclature

η_a	Absorbance efficiency (%)
λ	Wavelength (nm)
i	Incidence angle (degrees)
R	Reflection (%)
T	Transmission (%)
A	Absorption (%)
P	Radiant power (W)
I	Spectral irradiance ($W.m^{-2}.nm^{-1}$)

2. SPD switchable window

Switchable suspended particle windows use light absorptive rod-like particles in a water-like liquid between two Indium Tin Oxide (ITO) layers. In the opaque state, the randomly oriented particles absorb light. When a voltage is applied across the active layer, particles align with the electrical field reducing absorption giving a potentially transparent window. Typical transmission of 20-60%, 10-50% and 0.1-10% can be made by controlling the choice of absorptive particles, the particle density and the film thickness [1].

A switchable window with a total 9mm glass thickness and about 0.35mm active layer thickness provided by SmartGlass International has been tested [3]. The transmission spectra were recorded using a Lambda900 spectrophotometer 35cm in front of an integrating sphere. The transmission curves obtained are shown in figure 1.

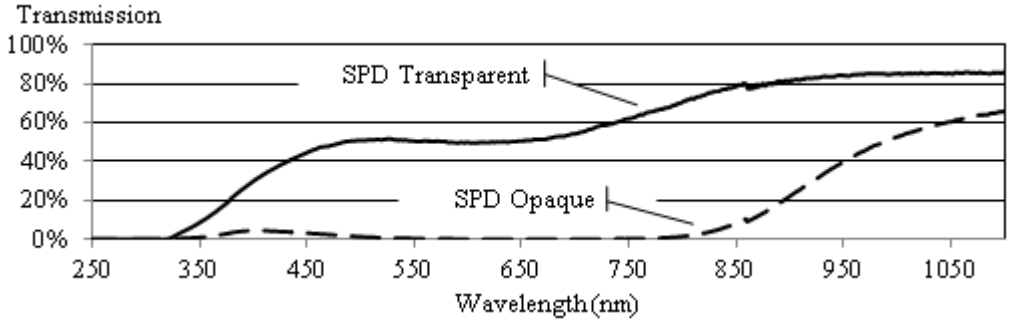

Fig. 1. SPD transmission in the opaque and transparent states

A UV filter is applied between the glass and ITO layers to protect the ITO layers from yellowing under UV radiations providing a cut-off wavelength of 330nm [3]. The average transmission in the UVB, UVA, visible and infrared light range up to 1100nm as well as the absorbance efficiency defined by equation 1 are calculated and provided in table 1.

$$\eta_a = \frac{T_{clear} - T_{opaque}}{T_{clear}} \quad (1)$$

Table 1. Transmission table of a SPD window in the clear and opaque states and the associated absorbance efficiency

		SPD Transmission		
		SPD clear	SPD opaque	η_a
Wavelength range	UVB (280-315nm)	0.08%	0.01%	87.57%
	UVA (316-399nm)	18.16%	3.05%	83.19%
	Vis (400-700nm)	48.54%	1.27%	97.37%
	IR (701-1100nm)	77.62%	27.43%	64.66%

A transmission of 48.5% in the clear state is however undesirably quite low for some applications. The type of rod-like particles may be changed or their density and the film thickness may be reduced to

further increase light transmission in the clear state while having more light transmitted in the opaque state. The infrared region is absorbed less efficiently with 27.4% average transmission of the light in the solar infrared range.

The SPD window currently allows a significant control of the visible light transmission and a reasonable control of the infrared. De-coupling the control of the visible and infrared transmission could be accomplished using two switchable windows; the first one would absorb the visible range and the second the infrared range. Note an electrochromic window made of tungsten oxide have been demonstrated to provide a peak near-infrared transmission modulation between 20% and 75% [1]. However if an SPD window (or using another switchable window technology) is made to further absorb the infrared light, this would imply unwanted heat absorption in the glazing reducing its lifetime, heat dissipation towards the back of the window and a fraction of the infrared heat wave re-radiated in the user's environment. Similarly to low-E glazing it is then preferable to reject infrared light. However, while low-E glazing have a determined reflection coefficient, CLC mirrors can efficiently modulate the amount of light rejection whilst still allowing independent control of the infrared transmission from the visible transmission.

3. CLC switchable mirrors

Chiral liquid crystal switchable mirrors can be tuned electronically between fully-reflective and fully-transmissive states applying a square waveform across the film. They can be manufactured to reflect light with a spectral bandwidth from 50nm to 1000nm, covering the visible and infrared range up to 3600nm.

The CLC switchable mirror experimentally characterized was a visible CLC mirror manufactured by Kent Optronics [8,9]. The mirror has two 2.5mm thick glass panes and a 20μm thick active layer. Reflection and transmission from the mirror were measured with a spectrophotometer. Reflection measurements were taken from 12 degrees to 62 degrees incidence angles in 4 degrees steps. Transmission measurements were also performed from 0 to 62 degrees in the same manner. The 'absorption' of the CLC mirror is defined as all light minus the combined measured reflection and transmission. This 'absorption' then accounts for multiple internal reflections of the light between the CLC interfaces.

The CLC mirror shows a significant variation of the spectral reflection and transmission with light incidence angle while the averaged absorption over 380-780nm remains constant at approximately 14.4% in the reflective state and 7.3% in the clear state. Spectral reflection, transmission and absorption curves in the reflective state are shown at 12 degrees incidence angle in figure 2 with 81.6% average reflection between 411nm and 718nm. Variation of the spectral reflection with light incidence is presented in figure3. Transmission light loss appears in the red spectral region (range B) as the incidence angle is increased while the reflection of the blue spectral range (range A) increases.

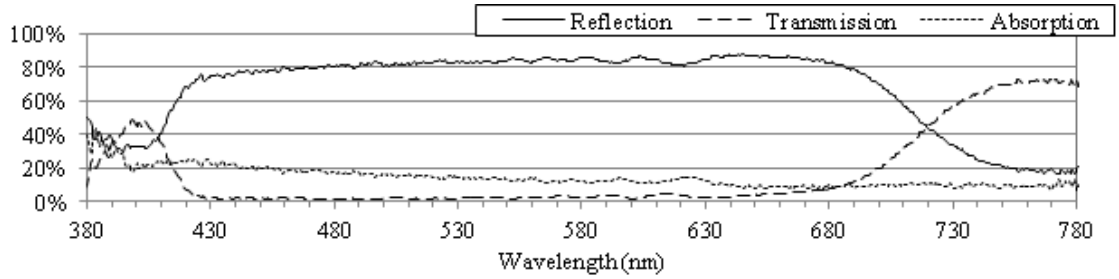

Fig. 2. CLC reflection, transmission and absorption at 12 degrees light incidence angle

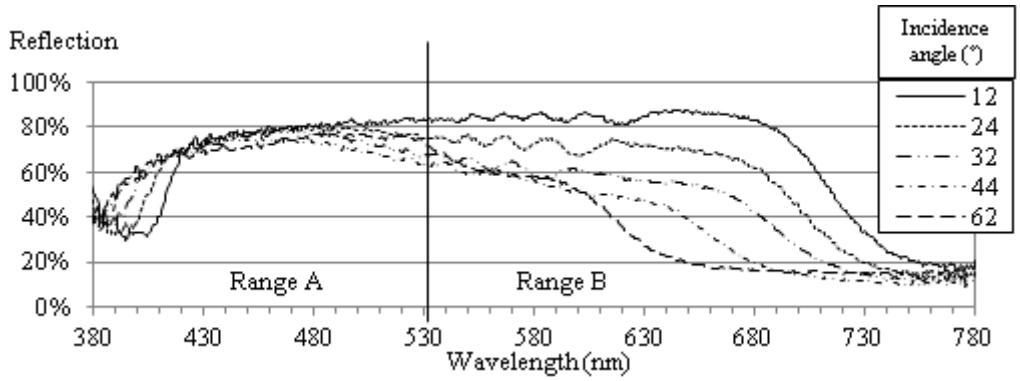

Fig. 3. CLC spectral reflection variation with light incidence angle in the reflective state

Quasi-full modulation of over 83% the design mirror reflectivity bandwidth occurs in a switching time of about 200ms seconds. In the clear state, the mirror transmission and reflection are approximately constant independently of the incidence angle. They are respectively equal to 84.3% and 8.4% up to 44 degrees incidence angle and therefore comparable to a single glass pane.

To simulate the performance of a double glazing window comprised of CLC mirrors independently of the incidence angle requires interpolation of the spectral reflection and transmission for any chosen angle. A linear interpolation was used for an angle between measured incidence angles. Outside that range, below 12 degrees in reflection and above 62 degrees both in reflection and transmission, the averaged reflection and transmission percentage curves and the reflection curve of unpolarized light at an air-glass interface are used to estimate the CLC layer reflection efficiency curve in the measured incidence angle. The last two data points, at 60 and 62 degrees are used to create a negative slope linear efficiency. The slope intercepts 0% efficiency at 90 degrees incidence. The extrapolation of the CLC reflectivity from 62 degrees to 90 degrees is then obtained by adding the contribution of air-glass interface reflectivity to the CLC angular reflection efficiency curve obtained, see figure 4. Considering a constant 14.4% absorption, the percentage average transmission curve with light incidence angle is calculated. To smooth the curves at the 62 degrees transition, a six-order polynomial function was obtained with a coefficient of determination R^2 over 99.7% both in reflection and transmission.

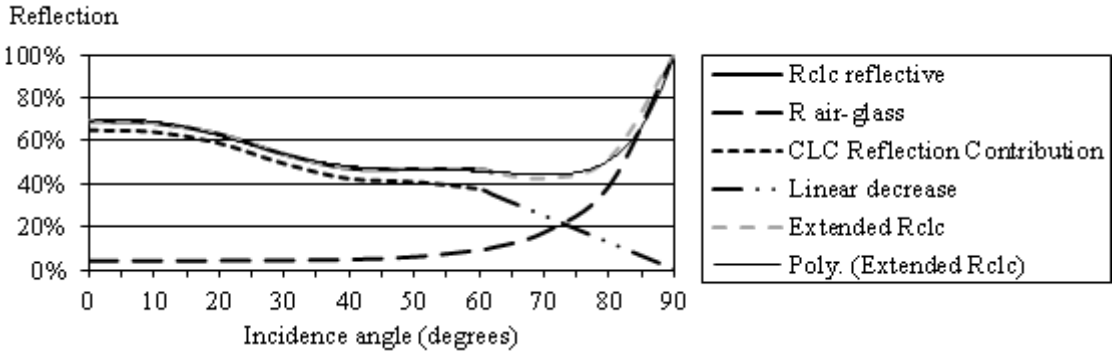

Fig. 4. Deriving the CLC contribution to reflection and extension of the reflection curve up to 90degrees incidence angle

In the clear state, the 7.3% absorption measured is used to calculate a linear coefficient of absorption of the CLC mirror of 0.143cm^{-1}. The CLC mirror behaved mostly like a single glazing, the reflection percentage at the air-glass and glass-air interfaces calculated to further obtain the total reflection of a single glazing with incidence angle. For all considered angles, the optical path length through the 0.5mm thick glazing is calculated to obtain the absorption curve and further on the average transmission curve. Similarly to the reflective state, six-order polynomial functions are obtained in reflection and transmission.

$$T_\lambda(i) = T_\lambda(62^\circ) * (1 + (\langle T\rangle_i - \langle T\rangle_{62})) \quad \text{for i > 62degrees} \tag{2}$$

Once the extrapolated curves were obtained from 0 to 90 degrees incidence angle, the reflection and transmission at a chosen wavelength and incidence angle is calculated by considering the closest known data point R(λ) at the incidence angle of 12 degrees or 62 degrees and T(λ) at 62degrees added by the percentage fluctuation obtained from the extrapolated averaged curves for the angle 'i' and either 12 or 62 degrees. Equation 2 expresses the calculated transmission at a wavelength λ and incidence angle 'i' above 62 degrees. A similar equation can be written in reflection for incidence angle below 0 degree and above 62 degrees. This method does not consider the wavelength shift with increased incidence angles.

4. Simulation method

The simulation program developed enables to create three-dimensional objects, assemble them to constitute the simulated system, creates a map of light points simulating the coverage of direct sun light with the desired vector direction according to solar angles and ray trace each beam of light. The presently considered system consists of two facing CLC mirrors with addressable pixels, followed by one SPD window. Although the hybrid window consists of infrared switchable mirrors, simulations are performed knowing the performance of the tested visible switchable mirror assuming an infrared mirror would perform equally. A beam containing wavelength from 400nm to 750 nm spaced at 10nm intervals with a reference power of 1W per wavelength is launched. Considering the vector direction of the beam, the next object reached by the beam and its interface is detected independently of the position and orientation of the objects. The incidence angle between the beam and the vector surface at the point of impact is calculated. The reflection state (fully transparent or fully reflective) of the pixel is then recognised and the reflection, transmission and absorption percentage of the mirror for all considered wavelength retrieved from the extrapolated data at the considered incidence angle. To limit the number of calculations, a beam that has its power coefficients at all wavelengths below 3% the original power of the light point source is discarded with the remaining fraction of light retained as heat at the pixel location of the intersected object. To simplify the model, a transmitted beam was considered as having the same vector direction as the incident beam within the object layer. The map of incident light source beams covering the entire window with each beam hitting individually different pixels, the total percentage of light reflected, absorbed and transmitted through the system as well as the percentage of light internally reflected and transferred to the photovoltaic cell are obtained for all scanned wavelengths and the given solar angles.

As the SPD switchable window was located behind the CLC mirrors, it does not need to be considered in the ray tracing to assess the performance of the two facing CLC mirrors. The absorption and transmission percentages of the SPD window can be further applied to the output of the CLC system to estimate the window final performances.

To provide a maximum of radiant light power falling onto the photovoltaic cell it is important to find the optimum configuration of reflective pixels to internally reflect the light down to the cell. To do so, a clear zone is left at the bottom of the window for the light to be incident on the photovoltaic cell either

directly or after one reflection on the back mirror. Once the height of the first clear area is determined, the heights of alternating reflective and transmissive areas are calculated considering a beam incident on the front mirror, reflecting on the back mirror and reaching the top of the previously calculated area on the front mirror. To minimize the number of internal reflections between mirrors, it is preferable to have the back mirror tilted with an angle as wide as possible. Considering the 50cm window height, a 4cm gap is introduce between the base of the mirrors, providing with an angle at their top of 4.57 degrees.

5. Results and discussion

The zenith angles considered were 20, 40 and 60 degrees. At an azimuth relative to the window of 0 degree, the performance of the system is first evaluated by turning-on the front CLC mirror to a transparent state while the back mirror is fully reflective. Changes of transmission, reflection and light collection are studied by introducing an azimuth angle of 30 degrees. Finally, areas of the front CLC mirror are set to a reflective state to assess the change of light collection using internal reflections. Spectral percentages of reflection, transmission, absorption from the system and percentage light on the photovoltaic cell are obtained using the ray-tracing simulation. Figure 5 shows the results for a zenith angle of 20 degrees at 0 degree azimuth angle (i.e. 70 degrees light incidence angle with the normal to the surface) with the front CLC mirror fully set to a transparent state while the back mirror is fully reflective.

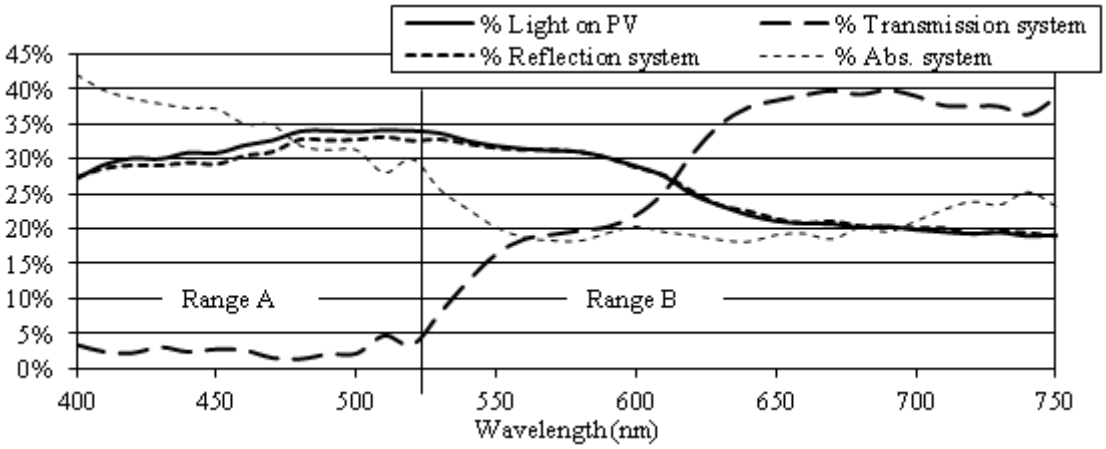

Fig. 5.Performance at 20 degrees zenith angle and 0 degree azimuth for a simulated window with the front CLC in the clear state and the back mirror fully reflective

It was assumed that an infrared CLC mirror reflecting light from 700nm to 1050nm would perform similarly to the measured and simulated CLC mirror reflecting the visible range. The infrared radiant power on the photovoltaic cell is calculated using the NREL standard solar irradiance $I(\lambda)$ at air-mass 1.5 [10] and the percentage of light transferred to the cell also representing the optical efficiency η_o of the window considered as a solar concentrator. The optical power loss from variations of the insolation and the efficiency of the photovoltaic cell were not considered.

Equations 3 to 6 are used to calculate the useful spectral power P_{useful} and the total power incident on the photovoltaic cell P_{PV}. The parameter A_{aw} represents the aperture area of the window of area A_w under a zenith angle θ and azimuth angle γ defined as the angle between the horizontal component of the beam

and the normal to the surface. To calculate the incident power on the window $P_{incident}$, integration over the wavelength step $\Delta\lambda$ of 10nm used during the simulation is considered. The total power collected on the cell is compared to what the cell would have collected in the considered solar angles without glazing. The cell being along the horizontal plane the aperture area of the cell A_{APV} is then described by equation 7 where A_{PV} is the area of the cell.

$$A_{aw} = A_w * \sin\theta * \cos\gamma \qquad P_{incident}(\lambda) = I(\lambda) * \Delta\lambda * A_{aw} \qquad (3)\ \&\ (4)$$

$$P_{useful}(\lambda) = P_{incident}(\lambda) * \eta_o(\lambda) \qquad P_{PV} = \sum P_{useful}(\lambda) \qquad (5)\ \&\ (6)$$

$$A_{APV} = A_{PV} * \cos\theta * \cos\gamma \qquad (7)$$

Table 2 and 3 provide the summary of the system performances according to the mirror configuration and solar angles. For the front mirror being fully transparent while the back mirror is fully reflective, 6.7W radiant power is collected at 20 degrees zenith in the 700-1050nm range considered. Naturally, the front mirror being transparent, reducing the incidence angle on the back mirror plane results in most of the light escaping the front window and the radiant power on the cell decreases. However, only 1.4W additional power to what the cell is directly collecting is provided by the back mirror at 20 degrees. Reflection increasing with decreasing incidence angle while the aperture area of the cell is simultaneously decreasing results in a small improvement of the additional power provided by the CLC back mirror up to 1.9W. Note that considering an ideal CLC mirror with its spectral reflection constant for all incidence angles and equal to its maximum value (at normal incidence) yields to 3.4W additional power at 20 degrees zenith and lowers down to 2.3W at 60 degrees zenith.

Table 2. Performances of the simulated system using equivalent IR CLC mirror to the characterized visible CLC mirror.

	System configuration							
Zenith (degrees)	20	40	60	20	40	60	20	20
Azimuth (degrees)	0	0	0	30	30	30	0	0
Number of mirror areas on front CLC - back CLC full mirror	0	0	0	0	0	0	2 CLC mirror	2 CLC clear
Average transmission over the covered range (%):	**20.4**	**28.2**	**26.7**	**18.1**	**28.0**	**30.1**	**18.8**	**32.9**
Average reflection over the covered range (%):	26.9	38.6	45.4	25.7	36.7	41.5	**50.2**	**21.4**
(Opt. Eff.) Average percentage of light transferred to PV (%):	26.7	13.1	7.7	27.9	14.6	8.4	13.5	19.6
Incident Power of Window (W)	23.9	45.0	60.6	20.7	39.0	52.5	23.9	23.9
Radiant Power on PV (W)	**6.7**	**6.2**	**4.7**	6.1	6.0	4.5	2.8	4.7
% power transferred to PV:	27.9	13.8	7.8	29.3	15.3	8.6	11.8	**19.6**
Radiant power directly incident on PV without glazing (W):	5.3	4.3	2.8	4.6	3.7	2.4	5.3	5.3
Energy concentration ratio:	1.3	1.4	1.7	1.3	1.6	1.9	0.5	0.9
Additional power provided by CLC mirrors (W):	**1.4**	**1.9**	1.9	**1.5**	**2.2**	2.1	-2.4	-0.6

Decreasing the zenith angle while maintaining the azimuth or increasing the azimuth angle while maintaining the zenith angle results in increasing the light incidence angle with the surface vector. The reflection change follows the extended reflection curve presented in figure 4. The CLC mirror in the reflective state, transmission continuously increases for incidence angle up to 40 degrees, flatten up to 75 degrees before continuously decreasing and reach 0% at 90 degrees. Reflection variation together with the increase of the incident light power when lowering the incidence angle explains the percentage of

transmission increases from 20 to 40 degrees zenith angle at 0 and 30 degrees azimuth and equivalent results at 40 and 60 degrees zenith angles.

Turning both front and back mirrors in the reflective state results in increasing the reflection. Transmission losses of the CLC mirror in the reflective state at high angles being significant, some light passes through the front and back mirrors resulting in 18.8% transmission. For both mirrors switched to their clear state, at 70 degrees incidence angle, an averaging 17.5% glazing reflectivity was considered in the visible range during the simulation resulting in the high 21.4% total reflectivity. The absorption resulting from multiple internal reflections within both CLC mirrors plays an important role in the consequent low 32% transmission. The 19.6% light transferred to the PV cell is then approximately equal to the ratio of the aperture area of the PV over the aperture area of the window minus the absorption by the front CLC. A narrower PV cell would results in lowering down this percentage while increasing the transmission percentage.

Table 3. System simulation results in the internally reflective configuration.

	System configuration					
Zenith (degrees)	20	40	60	20	40	60
Azimuth (degrees)	0	0	0	30	30	30
# of mirror area on front CLC - back CLC full mirror	**2**	**4**	**6**	**2**	**4**	**6**
Average transmission over the covered range (%):	20.1	25.4	22.3	18.0	25.1	26.6
Average reflection over the covered range (%):	32.3	40.3	48.2	33.0	40.3	43.3
(Opt. Eff.) Average percentage of light transferred to PV (%):	26.1	13.2	7.9	26.3	14.2	8.6
Incident Power of Window (W)	23.9	45.0	60.6	20.7	39.0	52.5
Radiant Power on PV (W)	6.5	6.3	4.9	5.6	5.8	4.7
% power transferred to PV:	27.2	13.9	8.1	27.2	14.8	9.0
Radiant power directly incident on PV without glazing (W):	5.3	4.3	2.8	4.6	3.7	2.4
Energy concentration ratio:	1.2	1.5	1.8	1.2	1.6	1.9
Additional power provided by CLC mirrors (W):	1.3	2.0	2.1	1.1	2.1	2.3
Power contribution provided by internal reflections (W):	**-0.2**	**0.1**	**0.2**	**-0.4**	**-0.2**	**0.2**

As shown in table 3, turning on areas of the front CLC mirror in the reflective state to internally reflect the light to the PV cell unfortunately results in having greater light rejection than additional power falling onto the cell at a low zenith angle. For high zenith angles, a small 0.2W additional power on the cell is provided by internal reflections. Simulations considering an ideal mirror with reflectivity maintained to the normal incidence value yields to only 0.7W power additional power by internal reflections at 60 degrees zenith. The additional power received on the cell is then mainly due to the bottom of the back mirror acting as a flat booster mirror. No benefit is then found in having two CLC mirrors to internally reflect the light onto a PV cell located in the frame of the window. It is therefore preferred to build a window with a front CLC mirror and back SPD window to solely independently control visible transmission and solar radiant heat transmission. The gap between panels could then be reduced resulting in increasing the percentage of transmission found during the simulation.

A system made of a front CLC infrared mirror and back SPD window would then be preferred to solely modulate the light transmission. The CLC-SPD system would then provide the combined results of the independently characterized CLC mirror and SPD window. In this case, considering a single CLC mirror, the significant transmission losses in the reflective state noted in range B of figure 3 would unwantedly show infrared transmission as high as 35% in range B of figure 5 when the sun is high in the sky. To avoid such issue it is most important to use a CLC mirror with a reflection bandwidth about 1.5 to

2 times wider than the wavelength range to modulate (700-1100nm). The expected average infrared transmission in the reflective state would be as low as 5% as seen in range A of figure 5 for all incidence angles. In the clear state, the CLC mirror is mostly equivalent to a single glazing and the infrared transmission could be higher than 84% minus ~3% absorption by the SPD glass panes at angles below 44 degrees. Reflection at the air-glass interface would rapidly increase above this angle. To maintain a high transmission of the clear state, an anti-reflective coating could be applied without affecting the desired reflection at the glass-active layer interface in the reflective state. Resulting solar radiant heat between ~80% and 5% transmission could be achieved.

The SPD window showed high absorbance efficiency in the visible range. However it would be required to use rod-like particles that solely absorb the visible range and appropriately adapt their density within the layer and/or the film thickness to increase the clarity of the window in the clear state. The solar heat radiation being rejected by the front CLC mirror rather than absorbed by the SPD window, long term heat damage on the system should be reduced. The front CLC mirror would need adaptation to outdoor and solar environments and mostly be protected from UV damage using UV filters transparent to the visible range as presently used in switchable windows. The current 200ms switching time of the CLC mirror does not need to be as fast in the infrared region as in the visible region since the user's comfort would not be directly affected. One can consequently consider a surrounding medium to the CLC molecules with a higher viscosity and permittivity [11]. Slowing down the rotational motion of the molecules would then possibly have the advantage to powering up the device at intermittent intervals or apply the required square waveform at a lower voltage. The average power consumption of the mirror would then possibly be reduced. A hybrid window using an infrared CLC mirror and SPD window would then independently and efficiently control solar radiant heat transmission, visible transmission and glare through the window.

Acknowledgements

The support of the Irish Higher Education Authority is acknowledged.

References

[1] Lampert, C. M. (1993). Optical switching technology for glazings. *Thin Solid Films*, *236*, 6-13.
[2] Lampert, C. M. (1995), Chromogenic Switchable Glazing: Towards the Development of the Smart Window. Window Innovations '95, Toronto, Canada, June 5-6, 1995,The Proceedings.
[3] SmartGlass International Ltd, SPD SmartGlass and LC SmartGlass. Available from: www.smartglassinternational.com.
[4] Karlson, J. (2001). Control system and energy saving potential for switchable windows. Seventh International IBPSA Conference, Rio de Janeiro,Brazil,August 13-15,2001.
[5] Griessen, R., Giebels, I. A. M. E. and Dam, B. (2004). *Optical properties of metal-hydrides: switchable mirrors*. Vrije Universiteit Amsterdam, Amsterdam.
[6] Richardson, T. J., Slack, J. L., Armitage, R. D., Kostecki, R., Farangis, B. and Rubin, M. D. (2001). Switchable mirrors based on nickel--magnesium films. *Applied Physics Letters*, *78*, (*20*), 3047-3049.
[7] Richardson, T. J., Slack, J. L., Armitage, R. D., Kostecki, R., Farangis, B. and Rubin, M. D. (2001). Switchable mirrors based on nickel--magnesium films. *Applied Physics Letters*, *78*, (*20*), 3047-3049.
[8] L. Li, "Single Layer Multi-State Ultra-Fast Cholesteric Liquid Crystal Device And The Fabrication Methods Thereof.". US Patent US 6,674,504 B1, 2004
[9] Kent Optronics Inc. e-TransFlector ™. Available from: http://www.kentoptronics.com/mirror.html.
[10]http://rredc.nrel.gov/solar/spectra/am1.5/
[11] H-Y Hsu, N. S., R S Ruoff and N A Patankar (2005). "Electro-orientation in particle light valves." Nanotechnology 16(2): 7.